Q-switched operation of a femtosecond-laser-inscribed Yb:YAG channel waveguide laser using carbon nanotubes

Sun Young Choi,[1] Thomas Calmano,[2,3] Mi Hye Kim,[1] Dong-Il Yeom,[1] Christian Kränkel,[2,3] Günter Huber,[2,3] and Fabian Rotermund[1,*]

[1]*Department of Energy Systems Research & Department of Physics, Ajou University, Suwon 443-749, South Korea*
[2]*Institut für Laser-Physik, Universität Hamburg, Hamburg 22761, Germany*
[3]*The Hamburg Centre for Ultrafast Imaging, Universität Hamburg, Hamburg 22761, Germany*
[*]*rotermun@ajou.ac.kr*

Abstract: We demonstrate a diode-pumped femtosecond-laser-inscribed Yb:YAG channel waveguide laser, *Q*-switched by using single-walled carbon nanotubes (SWCNTs) near 1029 nm. We used saturable absorber mirrors (SAMs) fabricated by depositing SWCNTs on three different output couplers. Best performance of the 9.3-mm-long ultra-compact *Q*-switched waveguide laser is obtained with an output coupling transmission of 20%. In this case, a maximum average output power of 60 mW with a corresponding pulse energy of 37.7 nJ and a pulse duration of 88 ns at 1.59-MHz repetition rate were achieved. The highest pulse energy of 39.2 nJ and the shortest pulse duration of 78 ns were obtained with 30% and 10% output couplers, respectively.

OCIS codes: (140.3615) Lasers, ytterbium; (140.3540) Lasers, *Q*-switched; (230.7380) Waveguides, channeled; (190.4400) Nonlinear optics, materials.

References and links

1. R. Aviles-Espinosa, G. Filippidis, C. Hamilton, G. Malcolm, K. J. Weingarten, T. Südmeyer, Y. Barbarin, U. Keller, S. I. C. O. Santos, D. Artigas, and P. Loza-Alvarez, "Compact ultrafast semiconductor disk laser: targeting GFP based nonlinear applications in living organisms," Biomed. Opt. Express **2**(4), 739–747 (2011).
2. Y. N. Billeh, M. Liu, and T. Buma, "Spectroscopic photoacoustic microscopy using a photonic crystal fiber supercontinuum source," Opt. Express **18**(18), 18519–18524 (2010).
3. S. Pekarek, T. Südmeyer, S. Lecomte, S. Kundermann, J. M. Dudley, and U. Keller, "Self-referenceable frequency comb from a gigahertz diode-pumped solid-state laser," Opt. Express **19**(17), 16491–16497 (2011).
4. R. J. Beach, S. C. Mitchell, H. E. Meissner, O. R. Meissner, W. F. Krupke, J. M. McMahon, W. J. Bennett, and D. P. Shepherd, "Continuous-wave and passively *Q*-switched cladding-pumped planar waveguide lasers," Opt. Lett. **26**(12), 881–883 (2001).
5. Y. E. Romanyuk, C. N. Borca, M. Pollnau, S. Rivier, V. Petrov, and U. Griebner, "Yb-doped $KY(WO_4)_2$ planar waveguide laser," Opt. Lett. **31**(1), 53–55 (2006).
6. J. I. Mackenzie and D. P. Shepherd, "End-pumped, passively *Q*-switched Yb:YAG double-clad waveguide laser," Opt. Lett. **27**(24), 2161–2163 (2002).
7. F. M. Bain, A. A. Lagatsky, S. V. Kurilchick, V. E. Kisel, S. A. Guretsky, A. M. Luginets, N. A. Kalanda, I. M. Kolesova, N. V. Kuleshov, W. Sibbett, and C. T. A. Brown, "Continuous-wave and *Q*-switched operation of a compact, diode-pumped Yb^{3+}:$KY(WO_4)_2$ planar waveguide laser," Opt. Express **17**(3), 1666–1670 (2009).
8. Y. Tan, A. Rodenas, F. Chen, R. R. Thomson, A. K. Kar, D. Jaque, and Q. Lu, "70% slope efficiency from an ultrafast laser-written Nd:$GdVO_4$ channel waveguide laser," Opt. Express **18**(24), 24994–24999 (2010).
9. J. Siebenmorgen, T. Calmano, K. Petermann, and G. Huber, "Highly efficient Yb:YAG channel waveguide laser written with a femtosecond-laser," Opt. Express **18**(15), 16035–16041 (2010).
10. T. Calmano, A.-G. Paschke, J. Siebenmorgen, S. T. Fredrich-Thornton, H. Yagi, K. Petermann, and G. Huber, "Characterization of an Yb:YAG ceramic waveguide laser, fabricated by the direct femtosecond-laser writing technique," Appl. Phys. B **103**(1), 1–4 (2011).
11. B. Charlet, L. Bastard, and J. E. Broquin, "1 kW peak power passively *Q*-switched Nd^{3+}-doped glass integrated waveguide laser," Opt. Lett. **36**(11), 1987–1989 (2011).

#234521 - $15.00 USD Received 12 Feb 2015; revised 13 Mar 2015; accepted 15 Mar 2015; published 19 Mar 2015

12. T. Calmano, J. Siebenmorgen, A. G. Paschke, C. Fiebig, K. Paschke, G. Erbert, K. Petermann, and G. Huber, "Diode-pumped high power operation of a femtosecond laser inscribed Yb:YAG waveguide laser," Opt. Mater. Express **1**(3), 428–433 (2011).
13. A. Choudhary, A. A. Lagatsky, P. Kannan, W. Sibbett, C. T. A. Brown, and D. P. Shepherd, "Diode-pumped femtosecond solid-state waveguide laser with a 4.9 GHz pulse repetition rate," Opt. Lett. **37**(21), 4416–4418 (2012).
14. R. Mary, G. Brown, S. J. Beecher, F. Torrisi, S. Milana, D. Popa, T. Hasan, Z. Sun, E. Lidorikis, S. Ohara, A. C. Ferrari, and A. K. Kar, "1.5 GHz picosecond pulse generation from a monolithic waveguide laser with a graphene-film saturable absorber output coupler," Opt. Express **21**(7), 7943–7950 (2013).
15. A. A. Lagatsky, A. Choudhary, P. Kannan, D. P. Shepherd, W. Sibbett, and C. T. A. Brown, "Fundamentally mode-locked, femtosecond waveguide oscillators with multi-gigahertz repetition frequencies up to 15 GHz," Opt. Express **21**(17), 19608–19614 (2013).
16. J. W. Kim, S. Y. Choi, D.-I. Yeom, S. Aravazhi, M. Pollnau, U. Griebner, V. Petrov, and F. Rotermund, "Yb:KYW planar waveguide laser *Q*-switched by evanescent-field interaction with carbon nanotubes," Opt. Lett. **38**(23), 5090–5093 (2013).
17. Y. Tan, S. Akhmadaliev, S. Zhou, S. Sun, and F. Chen, "Guided continuous-wave and graphene-based *Q*-switched lasers in carbon ion irradiated Nd:YAG ceramic channel waveguide," Opt. Express **22**(3), 3572–3577 (2014).
18. Y. Tan, C. Cheng, S. Akhmadaliev, S. Zhou, and F. Chen, "Nd:YAG waveguide laser *Q*-switched by evanescent-field interaction with graphene," Opt. Express **22**(8), 9101–9106 (2014).
19. A. Choudhary, S. Dhingra, B. D'Urso, T. L. Parsonage, K. A. Sloyan, R. W. Eason, and D. P. Shepherd, "*Q*-switched operation of a pulsed-laser-deposited Yb:Y_2O_3 waveguide using graphene as a saturable absorber," Opt. Lett. **39**(15), 4325–4328 (2014).
20. Y. Tan, Y. Yao, J. R. Macdonald, A. K. Kar, H. Yu, H. Zhang, and F. Chen, "Self-*Q*-switched waveguide laser based on femtosecond laser inscribed Nd:Cr:YVO_4 crystal," Opt. Lett. **39**(18), 5289–5292 (2014).
21. T. Calmano and S. Müller, "Crystalline Waveguide Lasers in the Visible and Near-Infrared Spectral Range," IEEE J. Sel. Top. Quantum Electron. **21**, 1602213 (2014).
22. T. Calmano, A. G. Paschke, S. Müller, C. Kränkel, and G. Huber, "Curved Yb:YAG waveguide lasers, fabricated by femtosecond laser inscription," Opt. Express **21**(21), 25501–25508 (2013).
23. Y. Jia, Y. Tan, C. Cheng, J. R. Vázquez de Aldana, and F. Chen, "Efficient lasing in continuous wave and graphene *Q*-switched regimes from Nd:YAG ridge waveguides produced by combination of swift heavy ion irradiation and femtosecond laser ablation," Opt. Express **22**(11), 12900–12908 (2014).
24. W. Bolaños, J. J. Carvajal, X. Mateos, E. Cantelar, G. Lifante, U. Griebner, V. Petrov, V. L. Panyutin, G. S. Murugan, J. S. Wilkinson, M. Aguiló, and F. Díaz, "Continuous-wave and *Q*-switched Tm-doped KY$(WO_4)_2$ planar waveguide laser at 1.84 μm," Opt. Express **19**(2), 1449–1454 (2011).
25. J. W. Szela, K. A. Sloyan, T. L. Parsonage, J. I. Mackenzie, and R. W. Eason, "Laser operation of a Tm:Y_2O_3 planar waveguide," Opt. Express **21**(10), 12460–12468 (2013).
26. K. M. Davis, K. Miura, N. Sugimoto, and K. Hirao, "Writing waveguides in glass with a femtosecond laser," Opt. Lett. **21**(21), 1729–1731 (1996).
27. Q. Bao, H. Zhang, Y. Wang, Z. Ni, Y. Yan, Z. X. Shen, K. P. Loh, and D. Y. Tang, "Atomic-laser graphene as a saturable absorber for ultrafast pulsed lasers," Adv. Funct. Mater. **19**(19), 3077–3083 (2009).
28. W. B. Cho, J. H. Yim, S. Y. Choi, S. Lee, A. Schmidt, G. Steinmeyer, U. Griebner, V. Petrov, D.-I. Yeom, K. Kim, and F. Rotermund, "Boosting the nonlinear optical response of carbon nanotube saturable absorber for broadband mode-locking of bulk lasers," Adv. Funct. Mater. **20**(12), 1937–1943 (2010).
29. H.-W. Yang, C. Kim, S. Y. Choi, G.-H. Kim, Y. Kobayashi, F. Rotermund, and J. Kim, "1.2-GHz repetition rate, diode-pumped femtosecond Yb:KYW laser mode-locked by a carbon nanotube saturable absorber mirror," Opt. Express **20**(28), 29518–29523 (2012).
30. S. Y. Choi, J. W. Kim, M. H. Kim, D.-I. Yeom, B. H. Hong, X. Mateos, M. Aguiló, F. Díaz, V. Petrov, U. Griebner, and F. Rotermund, "Carbon nanostructure-based saturable absorber mirror for diode-pumped 500-MHz femtosecond Yb:KLu$(WO_4)_2$ laser," Opt. Express **22**(13), 15626–15631 (2014).
31. J. A. Morris and C. R. Pollock, "Passive *Q* switching of a diode-pumped Nd:YAG laser with a saturable absorber," Opt. Lett. **15**(8), 440–442 (1990).

1. Introduction

Compact pulsed laser sources in the 1-μm spectral region are of particular interest for a variety of applications in microscopy, spectroscopy and metrology [1–3]. One of the important aspects for the development of compact laser systems is pumping with laser diodes. In recent years, Yb^{3+}- and Nd^{3+}-doped single crystals and ceramics exhibiting large emission cross sections, low quantum defects and low thermal loads turned out to be very promising candidates as gain media for the development of diode-pumped and highly efficient lasers both in continuous-wave (CW) and pulsed operation near 1 μm. Waveguiding structures allow for high intra-cavity pump intensities at reduced pump powers, an excellent overlap of the

#234521 - $15.00 USD Received 12 Feb 2015; revised 13 Mar 2015; accepted 15 Mar 2015; published 19 Mar 2015

pump and laser modes and efficient heat removal. To date, various CW and pulsed Yb^{3+}- and Nd^{3+}-doped solid-state lasers based on planar and channel waveguides are actively investigated [4–25]. In particular, the channel waveguide structures tend to deliver circular single-mode output in more efficient and stable operation due to an enhanced light confinement in small volumes. In addition e. g. to diffusion bonding, ion implantation and liquid-phase epitaxy [4,5,17], femtosecond-laser (fs-laser) inscription is a well-known technique for manufacturing channel waveguides inside dielectric gain materials. This relatively simple technique allows direct writing of straight and curved channels without masks [10,12,22,26]. Recently, diode-pumped high-power operation of a femtosecond-laser-inscribed Yb:YAG waveguide laser delivering CW output powers of up to 2.35 W was successfully demonstrated [12].

Q-switched or mode-locked pulsed waveguide lasers have been previously demonstrated using SESAMs, Cr-doped crystals, carbon nanotubes (CNTs) and graphene as saturable absorbers (SAs) in different schemes [13–21]. Intrinsic unique properties of carbon nanomaterials such as a broadband spectral applicability, a high nonlinearity, an ultrafast response time and the relatively simple manufacturing process [27–30] guarantee excellent performance of pulsed laser operation.

In this work, we report on single-mode diode-pumped fs-laser-inscribed Yb:YAG channel waveguide lasers, *Q*-switched by single-walled CNT SA mirrors (SWCNT-SAMs) for the first time. SWCNTs are deposited on different output couplers (OCs). The 9.3-mm-long laser cavity consists of an Yb:YAG waveguide and two mirrors (i.e., the end mirror and the output coupler (OC) acting simultaneously as a SAM) which are directly attached to both end-facets of the waveguide. In this configuration, operation characteristics using three SWCNT-deposited OCs of different transmissions (10%, 20% and 30%) are investigated.

2. Fabrication of channel waveguides and SWCNT-SAMs

The channel waveguides were fabricated by the fs-laser direct writing method [26] inside a 7% Yb^{3+}-doped YAG crystal using 150 fs pulses at a center wavelength of 775 nm from a 1 kHz Ti:sapphire chirped pulse amplifier (CPA) system (Clark-MXR CPA-2010). The fabrication process is described in detail in Ref. 22. The laser beam is focused with an aspheric lens (f = 3.1 mm) 345 μm below the polished surface of the Yb:YAG crystal and the tracks were written at a pulse energy of ~1.5 μJ. Two parallel tracks are written by moving the sample mounted on a motorized translation stage with a velocity of 25 μm/s, while the fs-laser beam is incident on the sample perpendicularly. The tracks inside the crystal induce stress which changes the refractive index in the material surrounding the tracks. The refractive index decrease of the tracks lead to a total refractive index change in the order of 10^{-3}-10^{-4} and this enables waveguiding between two written tracks. A separation of 28 μm between the tracks results in a good confinement of the fundamental mode near 1 μm [21]. The waveguide length after the polishing process is 9.3 mm.

To fabricate reflection-type SAs applicable for *Q*-switching of the Yb:YAG channel waveguide laser, arc-discharged SWCNTs (Meijo Carbon Co., Ltd) are used as starting material. The SWCNT powder is dissolved in 1,2-dichlorobenzene (o-DCB) at a concentration of 0.5 mg/ml and agitated for several hours in an ultrasonic bath. To remove metallic impurities and large bundles, the SWCNT dispersion is centrifuged for about 30 minutes. The well-dispersed SWCNT solution is then mixed with poly(methyl methacrylate) (PMMA) and the SWCNT/PMMA composite solution is spin-coated on different OCs to a layer thickness of about 300 nm. Finally, the coated OCs are used as SWCNT-SAMs in *Q*-switching experiments. It is noted that, for stable *Q*-switched operation of lasers, a larger modulation depth of the SA than for the case of mode-locking [29,30] is generally required. The fabricated SWCNT-SAMs used in the present work exhibit appropriate parameters for *Q*-switching. This was verified by measurements of the linear and nonlinear characteristics of SWCNTs deposited on fused silica substrate under identical conditions to those fabricated on

#234521 - $15.00 USD Received 12 Feb 2015; revised 13 Mar 2015; accepted 15 Mar 2015; published 19 Mar 2015

different OCs. The linear transmission of the SWCNT-SA is measured to be > 98% near the 1-μm region and a broad absorption band which arises from the E_{22} transition of the semiconducting SWCNTs appears around 1050 nm. The nonlinear transmission of the SWCNT-SA is measured at 1080 nm by employing a femtosecond Ti:sapphire laser-pumped optical parametric oscillator (OPO) with a resolution of 0.1%. The SWCNT-SA has a saturation fluence of < 40 μJ/cm^2, a modulation depth of 0.65% and nonsaturable losses of about 1%.

3. Experimental results

Figure 1 shows the experimental setup of the *Q*-switched Yb:YAG channel waveguide laser including the SWCNT-coated OC acting simultaneously as SAM. A single-mode pump beam from a can-type CW 940-nm laser diode (9-mm TO Can LD, Axcel photonics Inc.) is collimated using an aspheric lens of f = 6.24 mm. A Faraday isolator is inserted into the beam path to prevent back-reflection from the waveguide facets and the mirrors. A half-wave plate and a Glen-Taylor polarizer which is transparent for p-polarization are installed for pump beam attenuation by rotating the wave plate. The linearly p-polarized pump beam is focused onto the waveguide using a second aspheric lens (L1, f = 18.4 mm) through an incoupling mirror which is highly transparent at the pump wavelength and highly reflective at the laser wavelength. This mirror serves as an end mirror in the resonant cavity. The maximal CW pump power measured directly in front of the waveguide amounts to 264 mW. The 9.3-mm-long Yb:YAG channel waveguide as gain medium is mounted on a multiple-axis stage without active cooling. The SWCNT-deposited OC is then attached to the other end of the waveguide. Three different output coupling transmissions of 10%, 20% and 30% are investigated. For detection, a long-pass filter for filtering out the residual pump beam and a convex lens with f = 11 mm (L2) as a beam collimator are used outside the laser cavity. Figures 1(a) and 1(b) show the microscopic image of two 28-μm-separated tracks with the waveguide in between them and the top-view of this channel waveguide, respectively. The depth of tracks from the crystal surface is about 345 μm. As shown in Fig. 1(c), the end mirror and SWCNT-coated OC are directly attached to each end-facet, and hence, the total cavity length of the *Q*-switched Yb:YAG channel waveguide laser is determined by the length of the gain medium, i.e., 9.3 mm. To prevent Fresnel losses and undesired feedback, index matching oil is used between both waveguide facets and mirrors.

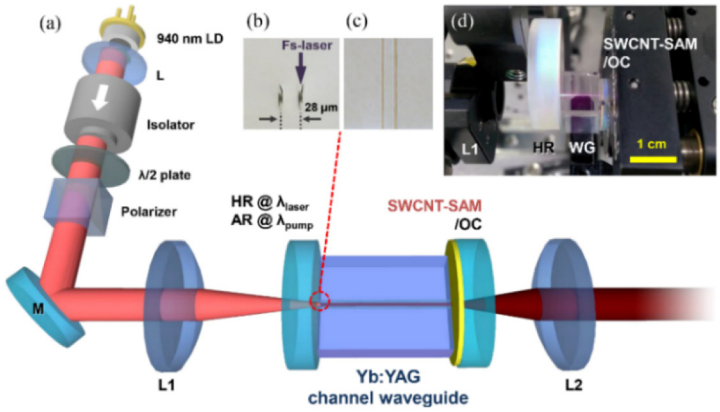

Fig. 1. (a) Experimental setup of *Q*-switched Yb:YAG channel waveguide laser with SWCNT-coated output coupler. L: aspheric lens with f = 6.24 mm, λ/2 plate: half-wave plate, isolator: Faraday isolator, polarizer: Glen-Taylor polarizer, M: bending mirror, L1: aspheric lens with f = 18.4 mm, OC: 10%, 20% or 30% output coupler, L2: convex lens with f = 11 mm. Insets; Microscope images of (b) cross-section of the femtosecond-laser-inscribed two 28-μm-separated tracks and (c) top-view of the Yb:YAG channel waveguide. (d) Photograph of the laser setup.

#234521 - $15.00 USD Received 12 Feb 2015; revised 13 Mar 2015; accepted 15 Mar 2015; published 19 Mar 2015

First, CW operation of the Yb:YAG channel waveguide is investigated in different cavity configurations. Figure 2(a) shows the laser characteristics for three different setups in the CW regime. The fabricated waveguide itself can be used as a resonant cavity without mirrors, since both waveguide facets act as a Fabry-Perot resonator [9]. Although the waveguide emits the laser beam both in backward and forward directions, the output power is only measured in forward direction as shown in Fig. 2(a). The lasing threshold in this case is 135 mW with a slope efficiency of only 24%. However, as reported in Ref. 9, the output power in backward direction is usually in the same order. Thus, a doubled forward direction output efficiency is expected by preventing backward direction output with appropriate mirrors. Therefore, we extend the laser setup to a configuration with a high-reflection end mirror (HR-WG) serving simultaneously as the incoupling mirror of the pump beam (inset of Fig. 2(a)). In this case the lasing threshold is decreased to 79 mW and a slope efficiency of 49% is measured, which is in good agreement with the prediction from the results for the waveguide with only Fresnel feedback. The maximum output power in this HR-WG geometry is 90 mW at 264-mW pump power. Figure 2(b) shows the CW output characteristics of the final laser setup with OCs of T = 10%, 20% and 30% without SWCNT-coating. The laser emission starts from a pump power of less than 50 mW in all cases. The slope efficiencies decrease for lower output coupler transmission due to the lower resonator extraction efficiency and are estimated to be 25%, 33% and 35% for T = 10%, 20% and 30%, respectively. The maximum output power of 74 mW is achieved with T = 30% at 264 mW of pump power. The CW laser spectra with different OCs are nearly identical. The laser spectrum is centered at 1028.5 nm with a spectral bandwidth of about 0.6 nm.

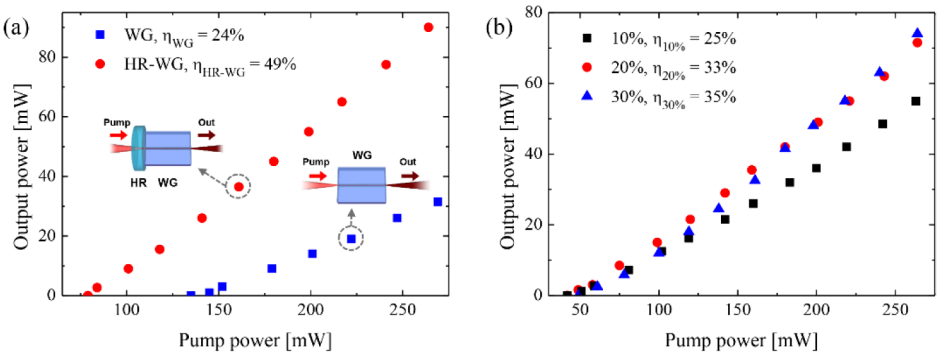

Fig. 2. CW laser operation of an Yb:YAG channel waveguide laser in different configurations: (a) output power characteristics from the waveguide end-facets as resonant cavity (blue squares) and the waveguide with a high-reflection end mirror (red dots) and (b) output power characteristics with three different output coupler transmissions (10%, 20% and 30%).

Q-switched operation of the Yb:YAG channel waveguide laser is subsequently demonstrated by adding OCs with SWCNT coating. The SAM-OC is mounted on a 2-axis translation stage enabling us to find optimal positions for sufficient saturable absorption. Above the lasing threshold which is comparable to the CW case, stable *Q*-switched operation is easily achieved. Figure 3 shows the output characteristics in the *Q*-switched regime. Figure 3(a) shows the measured average output powers for the different SWCNT-coated OCs. The maximum average output power of 60 mW and the highest slope efficiency of 28% are achieved with T = 20%. For T = 10% and T = 30%, the average output power increases linearly with the pump power with slope efficiencies of 21% and 27%, respectively. The slight decrease in output powers compared to the CW operation with uncoated OCs is mainly attributed to additional cavity losses caused by the SWCNT-SAs. The sensitivity of the output power and repetition rate towards transversal alignment of the SWCNT-coated OCs is low and stable *Q*-switched operation is maintained. This indicates the homogeneous surface

#234521 - $15.00 USD Received 12 Feb 2015; revised 13 Mar 2015; accepted 15 Mar 2015; published 19 Mar 2015

quality of the SWCNT-coating. The *Q*-switched channel waveguide laser shows a pump-power-dependent behavior which is similar to that typically observed in lasers passively *Q*-switched with saturable absorbers [31]. By increasing the pump power, the repetition rate and pulse energy increase, while the pulse duration decreases (Figs. 3(b) and 3(c)). The repetition rate with the SWCNT-coated 10% and 20% OCs can be tuned between about 1 and 1.6 MHz depending on the pump power, whereas it varies between about 0.8 and 1.4 MHz with the 30% OC, as shown in Fig. 3(b).

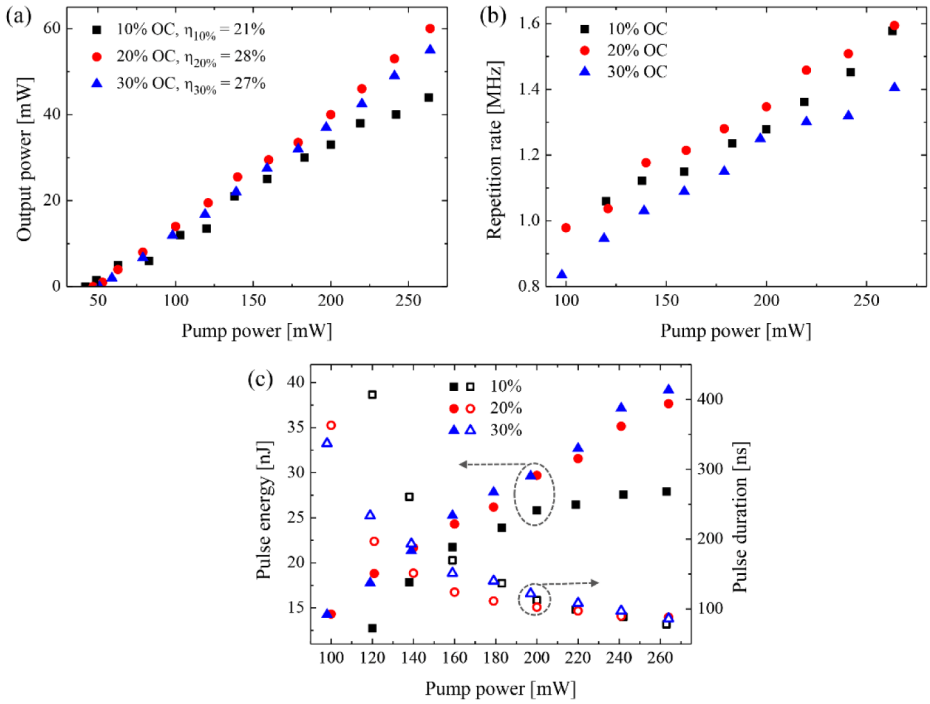

Fig. 3. Yb:YAG channel waveguide laser *Q*-switched by SWCNT-coated OCs: (a) average output power characteristics and (b) repetition rates for three different output couplers. (c) Pulse width and (d) pulse energy as function of incident pump power for 20% OC

In Fig. 4(a), an exemplary laser spectrum and pulse shape (upper inset) for 20% output coupling are depicted. The lower inset shows the beam profile of the output beam with a nearly circular fundamental mode recorded by a beam profiler (LaserCam-HR, Coherent Inc.). The output beam diameter measured after collimation in a distance of about 30 cm from OC is 0.4 mm. The *Q*-switched laser operates also near 1029 nm for the other output coupler transmissions and the beam modes are very similar in all cases such as in the case of CW operation. The shortest pulse duration and the maximum pulse energy are measured with the 10% and 30% OCs to be 78 ns and 39.2 nJ, respectively, at the maximum-available pump power of 264 mW. It should be noted that in contrast to many other *Q*-switched waveguides the pulses are fully modulated. Moreover, the stability of *Q*-switching was excellent, which was confirmed by measurements of the pulse train in different time-spans (Fig. 4(b)). Although the waveguide is not externally cooled, the *Q*-switching is stable for hours with negligible changes. Furthermore, the application of a laser diode as a pump source paves the way towards a further miniaturization of crystalline pulsed active optical devices.

#234521 - $15.00 USD Received 12 Feb 2015; revised 13 Mar 2015; accepted 15 Mar 2015; published 19 Mar 2015

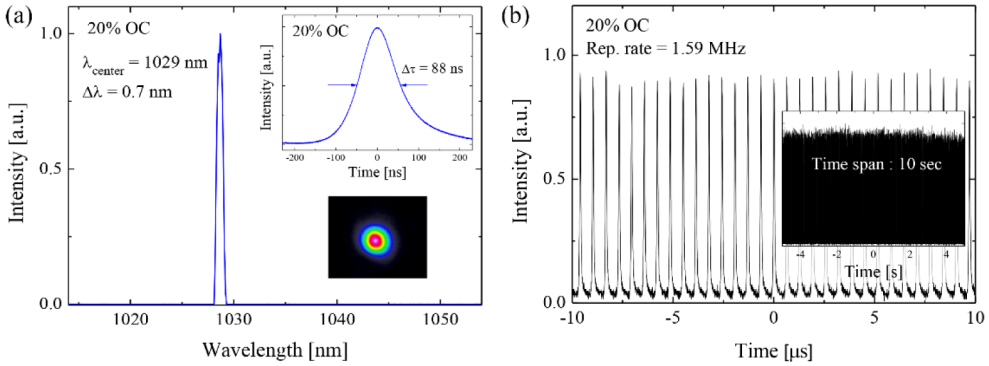

Fig. 4. Yb:YAG channel waveguide laser *Q*-switched with SWCNT-coated 20% OC: (a) laser spectrum, beam profile (lower inset) and pulse shape (upper inset), and (b) measured pulse train in different time-spans of 20 μs and 10 s.

4. Conclusion

We report the first diode-pumped femtosecond-laser-inscribed Yb:YAG channel waveguide laser, *Q*-switched by SWCNT-coated output couplers. The channel waveguide created between two precisely fs-laser-inscribed parallel tracks delivers a spatially circular fundamental-mode both in CW and *Q*-switched regimes. Using SWCNT-coated different output couplers acting simultaneously as saturable absorber mirrors in the present laser setup, *Q*-switched operation characteristics of a 9.3-mm-long ultra-compact laser is systematically investigated. High transmission, low saturation fluence and suitable modulation depth of SWCNT-SAMs enable us to generate stable *Q*-switched pulses. Improvements of the laser performance including higher output power, shorter pulse duration and even mode-locked operation at GHz repetition rates should be possible by applying higher pump powers, dispersion compensation and fine control of the saturable absorber parameters. This work is currently in progress.

Acknowledgments

This work was supported by the National Research Foundation of Korea (NRF) Grants funded by Korea Government (MEST and MSIP) (2011-0017494 and WCI 2011-001). This work was also partially supported by the Center for Advanced Meta-Materials (CAMM) funded by Korea Government (MSIP) as Global Frontier Project (CAMM 2014M3A6B3063709). Moreover, we acknowledge funding by the Deutsche Forschungsgemeinschaft in the framework of the project FKZ CA 1380/1-1 and the excellence cluster 'The Hamburg Centre for Ultrafast Imaging - Structure, Dynamics and Control of Matter at the Atomic Scale'.